

Periodic event-triggered impulsive control for fully heterogeneous stochastic multi-agent systems with a time-varying topology

Xuetao Yang, Ruilu An, Quanxin Zhu*, *Senior Member, IEEE*

Abstract—In this paper, we focus on a periodic event-triggered impulsive control (PETIC) for fully heterogeneous stochastic multi-agent systems (MASs) with a time-varying topology. Firstly, a novel time-varying topology is established by incorporating the energy consumption of each agent. This topology enables active adjustment of the information interaction intensity between agents. Secondly, to address the difficulties that agents with different dimensions cannot communicate in fully heterogeneous stochastic MASs, a virtual state space is designed. According to the above framework, novel PETICs with/without actuation delays are presented to achieve the mean-square exponential consensus of fully heterogeneous stochastic MASs. Finally, the effectiveness of the proposed methods is verified through a numerical simulation of unmanned aerial vehicles and unmanned ground vehicles.

Index Terms—Full heterogeneity, stochastic multi-agent systems, time-varying topology, event-triggered impulsive control, mean-square exponential consensus.

I. INTRODUCTION

IN recent years, multi-agent systems (MASs) have attracted remarkable attention due to their extensive applications in engineering fields such as unmanned aerial vehicle motion, smart grids, robot control and so on (see, e.g., [1], [2], [3]). One of the core issues underlying the effective operation of multi-agent systems is the consensus problem, which enables all agents to achieve a common task objective by receiving information from their adjacent agents (see, e.g., [4], [5]). Due to the importance of the consensus problem, it has gradually become a popular topic, which promotes our research.

In engineering practice, the condition that all agents have identical models exhibits significant limitations, which has driven the development of heterogeneous MASs. It is worth noting that most heterogeneous MASs primarily differ in the rules governing each agent's state evolution, while differences in agents' dimensions are often overlooked (see, e.g., [6], [7], [8], [9], [10]). This observation has aroused our research interest in fully heterogeneous MASs with agents of different dimensions. However, differences in agents' dimensions

This work was jointly supported by the National Natural Science Foundation of China (62173139).

Xuetao Yang is with School of Science, Nanjing University of Posts and Telecommunications, Nanjing 210023, Jiangsu, China, and also with MOE-LCSM, School of Mathematics and Statistics, Hunan Normal University, Changsha 410081, Hunan, China.

Ruilu An is with School of Science, Nanjing University of Posts and Telecommunications, Nanjing 210023, Jiangsu, China.

Quanxin Zhu is with MOE-LCSM, School of Mathematics and Statistics, Hunan Normal University, Changsha 410081, China (The corresponding author is Quanxin Zhu with email: zqx22@126.com).

create obstacles to information transmission between agents. Therefore, it is a challenge to achieve consensus in fully heterogeneous MASs. In [11], a dynamic compensator is constructed for each agent to receive and transmit information. In [12], a distributed observer is proposed to estimate the states of follower systems and to ensure information transmission between followers. However, the aforementioned fully heterogeneous MASs are all deterministic systems. For fully heterogeneous stochastic MASs, the stochastic noise is unobservable, which leads to the methods applicable to deterministic systems infeasible. Thus, for fully heterogeneous stochastic MASs, how to enable agents to overcome dimensional differences and achieve consensus is one of the key problems addressed in this paper.

Currently, the topological structures in most studies are static, which means that fixed communication is always maintained between agents (see, e.g., [13], [14], [15], [16]). However, in reality, due to factors such as environmental changes, the agents' own conditions and task requirements, the information interaction between agents changes over time. In dynamic topological scenarios, controllers designed for static topologies often lose their effectiveness because they cannot adapt to the time-varying communication relationships between agents. To address this issue, some studies have proposed controllers based on switching topologies (see, e.g., [17], [18], [19]). Nevertheless, the switching modes employed in these methods are limited and preconfigured. In this paper, we are devoted to designing a time-varying topology that adapts to the individual characteristics of agents, which facilitates MASs in achieving its task objectives. Energy is a fundamental requirement for the stable operation of agents (see, e.g., [20], [21], [22]). When energy is insufficient, the risk of agent instability increases significantly. Therefore, it is essential to design an energy-adaptive dynamic topological structure. Then, how to design a control strategy with an energy-adaptive dynamic topology has become an urgent problem that needs solving.

During the past several years, impulsive controls have attracted widespread attention due to its characteristics of simple design and easy implementation. Traditional impulsive controls are triggered based on time (see, e.g., [23], [24], [25]). However, event-triggered impulsive controls (ETICs) can provide flexible updating times for the controller based on an event-triggering mechanism (ETM) (see, e.g., [26], [27], [28], [29], [30]). So, ETICs can significantly reduce bandwidth consumption and they have been extensively applied in many systems such as complex networks, switched systems and

coupled neural networks (see, e.g., [31], [32], [33], [34]). Therefore, we are committed to applying ETICs to fully heterogeneous stochastic MASs.

In the scenario of time-varying topology, we combine an energy consumption function with periodic ETM (PETM) and propose a novel periodic ETIC (PETIC). The advantage is that this novel PETIC can not only solve the consensus problem of stochastic MASs, but also avoid the Zeno phenomenon effectively. Meanwhile, to account for the impact of actuation delays (i.e., the delays occurring between the controller and the actuator), we also propose a novel PETIC with actuation delays. The significant contributions of this paper are summarized as follows:

- 1) To address the issue of different states' dimensions in fully heterogeneous stochastic MASs, a novel virtual state space is introduced, which ensures the transmission of information between agents. Moreover, the virtual system states can be effectively degenerated into the original system states.
- 2) Different from the topologies proposed in [13], [14], [15], [16], [17], [18], [19], we establish a novel time-varying topology based on energy. By incorporating the energy consumption of each agent into the topology, the information transmission between adjacent agents is more adaptive to the individual characteristics of each agent.
- 3) Two kinds of novel PETICs are proposed. Different from the fixed updating instants of impulsive controls (see, e.g., [23], [24], [25]), control updating instants considered in this paper are a sequence of stopping times selected by PETM, which save communication resources more reasonably. Meanwhile, unlike traditional PETMs based on system states directly (see, e.g., [26], [27], [30]), our PETM is based on virtual states, which is more suitable for fully heterogeneous systems. Furthermore, energy consumption designed in PETICs plays a positive role in accelerating the consensus rate of stochastic MASs.

This paper is structured as follows. In Section II, we introduce a fully heterogeneous stochastic MAS with a time-varying topology. In Section III, we propose PETICs with/without actuation delay strategies to ensure system consensus. In Section IV, we provide the simulation results for unmanned aerial vehicles (UAVs) and unmanned ground vehicles (UGVs). In the final section, we wrap up the paper with some conclusions.

II. PROBLEM FORMULATION

A. Notations

Let $\mathbb{N} = \{0, 1, \dots\}$ and $\mathbb{N}^+ = \{1, 2, \dots\}$. For a real square matrix M , $\lambda_{\max}(M)$ and $\lambda_{\min}(M)$ denote the largest and smallest eigenvalues, respectively. $|M|$ represents the Euclidean norm. For real square matrices M_1 and M_2 , $M_1 \otimes M_2$ is the Kronecker product of the matrices M_1 and M_2 . For constants a, b and c , $\text{diag}\{a, b, c\}$ denotes a square matrix with diagonal elements a, b and c , while all other elements are zero. Furthermore, define $a \vee b = \max\{a, b\}$. I_n refers to the

identity matrix of dimension n . $\mathbf{0}$ is a dimension-compatible zero matrix. $\omega(t)$ is a standard Wiener process defined on a complete probability space $(\Omega, \mathcal{F}, \{\mathcal{F}_t\}_{t \geq 0}, \mathcal{P})$, in which the filter $\{\mathcal{F}_t\}_{t \geq 0}$ satisfies the usual conditions.

B. Time-varying Graph Theory

For a positive integer N , let $\mathcal{N} = \{1, 2, \dots, N\}$. In this paper, $\tau_i(t)$, $i \in \mathcal{N}$ represents the energy consumption of each agent (see [20] for instance). We incorporate $\tau_i(t)$ into the communication topology. Then, the communication topology of followers is described as a directed graph $\mathcal{G}(t) = (\mathbb{V}, \mathcal{E}(t), \mathcal{A}(t))$ with the set $\mathbb{V} = \{v_1, v_2, \dots, v_N\}$, the edge set $\mathcal{E}(t) \subseteq \mathbb{V} \times \mathbb{V}$ and the weighted adjacency matrix $\mathcal{A}(t) = [a_{ij}(t)]_{N \times N}$, where $a_{ij}(t) = \bar{a}_{ij}e^{-\alpha\tau_i(t)}$, \bar{a}_{ij} and α are positive constants. The neighbors of agent i at instant t are depicted as $\mathcal{N}_i(t) = \{j \in \mathbb{V} | (j, i) \in \mathcal{E}(t)\}$. The Laplacian-like matrix of $\mathcal{G}(t)$ is given as $\mathbb{L} = [\bar{a}_{ij}]_{N \times N}$ with $\bar{a}_{ii} = \sum_{j \neq i} \bar{a}_{ij}$ and $\bar{a}_{ij} = -\bar{a}_{ji}$, $i \neq j$. If the matrix $\mathcal{G}(t)$ has a leader, then the diagonal matrix $\mathcal{B}(t) = [b_i(t)]_{N \times N} = \text{diag}\{\bar{b}_1e^{-\alpha\tau_1(t)}, \bar{b}_2e^{-\alpha\tau_2(t)}, \dots, \bar{b}_Ne^{-\alpha\tau_N(t)}\}$ can be used to represent the connectivity between leaders and followers, where \bar{b}_i is a non-negative constant. We define a matrix $B = \text{diag}\{\bar{b}_1, \bar{b}_2, \dots, \bar{b}_N\}$ and an information-exchange matrix $H = -\mathcal{L} + B$, where B is not a zero matrix.

Assumption 1: Suppose that the energy consumption $\tau_i(t)$ is independent of the system states $x_0(t)$, $x_i(t)$, $z_i(t)$ and $y_i(t)$, which will be determined later by (1), (2), (3), and (5).

Remark 1: Different from the traditional static communication topologies (see, e.g., [13], [14], [15], [16]), this paper explicitly considers the influence of energy consumption on information interaction between adjacent agents. To capture this impact, the novel time-varying weighted adjacency matrix $\mathcal{A}(t)$ and a diagonal matrix $\mathcal{B}(t)$ are presented. Then, topology structure under different energy consumption scenarios is as follows:

- 1) When $\tau_i(t) = 0$, the weights $a_{ij}(t) = \bar{a}_{ij}$ and $b_i(t) = \bar{b}_i$. That is to say, when an agent has sufficient energy, the topology assigns the agent the maximum communication weight. At this point, $\mathcal{G}(t)$ degenerates into a static topology \mathcal{G} , which is consistent with traditional communication graphs.
- 2) When $0 < \tau_i(t) < +\infty$, the weights $a_{ij}(t)$ and $b_i(t)$ decrease as $\tau_i(t)$ increases. The more energy an agent consumes, the less capability it has to receive information transmitted by other agents. This dynamic variation also prevents high-energy-consumption agents from undertaking excessive communication and coordination tasks.
- 3) When $\tau_i(t) \rightarrow +\infty$, the weights $a_{ij}(t) \rightarrow 0$ and $b_i(t) \rightarrow 0$. That is, when an agent runs out of energy, it is automatically removed from the topological structure.

C. A fully heterogeneous stochastic MAS

Take into account the leader state below

$$\begin{aligned} dx_0(t) &= [C_0 x_0(t) + f_{x0}(x_0(t))] dt \\ &\quad + D_0 x_0(t) d\omega(t), \quad t > 0, \end{aligned} \quad (1)$$

where $x_0(t) \in \mathbb{R}^{n_0}$ is the leader state with an initial value $x_0(0) \in \mathbb{R}^{n_0}$. $C_0 \in \mathbb{R}^{n_0 \times n_0}$ and $D_0 \in \mathbb{R}^{n_0 \times n_0}$ are constant matrices. $f_{x_0}(\cdot) : \mathbb{R}^{n_0} \rightarrow \mathbb{R}^{n_0}$ is a continuous function.

Meanwhile, consider the following stochastic MAS of N agents:

$$\begin{aligned} dx_i(t) = & [C_i x_i(t) + f_{x_i}(x_i(t)) + u_i(t)]dt \\ & + D_i x_i(t) d\omega(t), \quad i \in \mathcal{N}, \quad t > 0, \end{aligned} \quad (2)$$

where $x_i(t) \in \mathbb{R}^{n_i}$ represents the i -th system state with an initial value $x_i(0) \in \mathbb{R}^{n_i}$. $u_i(t) \in \mathbb{R}^{n_i}$ stands for a control input. $C_i \in \mathbb{R}^{n_i \times n_i}$ and $D_i \in \mathbb{R}^{n_i \times n_i}$ are system matrices. $f_{x_i}(\cdot) : \mathbb{R}^{n_i} \rightarrow \mathbb{R}^{n_i}$ is a continuous function. Next, to solve the consensus problem of the leader-following system, we propose the following assumption.

Assumption 2: Suppose that there exists a matrix $\Xi_i \in \mathbb{R}^{n_i \times n_0}$ such that $\Xi_i C_0 = C_i \Xi_i$ and $\Xi_i D_0 = D_i \Xi_i$.

Remark 2: Assumption 1 is a classical condition for heterogeneous leader-following systems (see, e.g., [11], [12]).

Let $z_i(t) = x_i(t) - \Xi_i x_0(t)$ with the initial value $z_i(0) = x_i(0) - \Xi_i x_0(0)$. Under Assumption 2, systems (1) and (2) can be rewritten as

$$\begin{aligned} dz_i(t) = & [C_i z_i(t) + f_i(z_i(t)) + u_i(t)]dt \\ & + D_i z_i(t) d\omega(t), \quad i \in \mathcal{N}, \quad t > 0, \end{aligned} \quad (3)$$

where $f_i(z_i(t)) = f_{x_i}(x_i(t)) - \Xi_i f_{x_0}(x_0(t))$. Subsequently, one assumption regarding system (3) are presented.

Assumption 3: Suppose that $f_{x_0}(x_0(t))$, $f_{x_i}(x_i(t))$ and $f_i(z_i(t))$ satisfy the Lipschitz condition with $f_{x_0}(0) = 0$, $f_{x_i}(0) = 0$ and $f_i(0) = 0$. Moreover, there exists a non-negative constant L_{f_i} such that $|f_i(z_i(t))| \leq L_{f_i} |z_i(t)|$.

Remark 3: Under Assumption 3, it follows from [35] that system (3) has a unique global solution.

D. Virtual state space

To solve the problem of different state dimensions in the fully heterogeneous stochastic MAS, we construct a state space with m dimensions. Then, the virtual state $y_i(t)$ satisfies

$$y_i(t) = \Phi_i z_i(t), \quad i \in \mathcal{N}, \quad (4)$$

where $\Phi_i \in \mathbb{R}^{m \times n_i}$ is a constant matrix and $m \geq n_i$. In the following, we present a necessary assumption to guarantee the effectiveness of the virtual state space.

Assumption 4: Suppose that matrix Φ_i satisfies $\text{rank}(\Phi_i) = n_i$. Moreover, there exists a matrix $\Theta_i \in \mathbb{R}^{n_i \times m}$ such that $\Theta_i \Phi_i = I_{n_i}$.

Remark 4: Under Assumption 4, it follows from formula (4) that $z_i(t) = \Theta_i y_i(t)$. The existence of matrix Θ_i implies that the original state $z_i(t)$ can be exactly reconstructed from the virtual state $y_i(t)$ via a fixed linear transformation. Consequently, embedding the original states of heterogeneous systems into an m -dimensional virtual state space does not lead to any loss of state information.

Remark 5: The necessity for an m -dimensional virtual state space to be constructed is stated as follows: On the one hand, compared with [11] and [12], system (3) includes unobservable stochastic noise. On the other hand, the condition $m \geq n_i$ is

required to preserve all information in the following systems. If each follower is directly mapped to the leader's dimension, it cannot cover the application scenarios when $n_0 < n_i$. Therefore, we design the virtual state space, which not only eliminates the need to observe stochastic noise but also covers all application scenarios of leader-follower systems.

According to system (3) and formula (4), we obtain the virtual stochastic MAS

$$\begin{aligned} dy_i(t) = & [\Phi_i C_i \Theta_i y_i(t) + \Phi_i f_i(t) + \Phi_i u_i(t)]dt \\ & + \Phi_i D_i \Theta_i y_i(t) d\omega(t), \quad i \in \mathcal{N}, \quad t > 0, \end{aligned} \quad (5)$$

where $f_i(t) = f_i(\Theta_i y_i(t))$ and $y_i(0) = \Phi_i z_i(0)$ denotes the initial value of the state $y_i(t)$.

III. MAIN RESULTS

In this section, we investigate PETIC for a stochastic MAS with time-varying topology, as illustrated in Fig. 1. Specifically, we consider two cases: a controller without actuation delays and a controller with actuation delays.

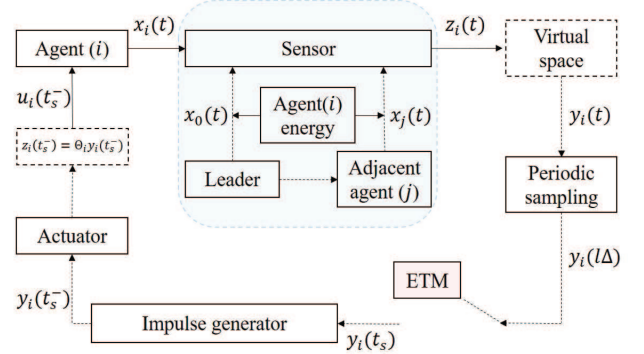


Fig. 1. Configuration of a stochastic MAS with time-varying topology.

A. PETIC

In order to reduce the consumption of control resources, the impulsive controller is designed as

$$u_i(t) = \sum_{s=0}^{\infty} k_i U_i(t) \delta(t - t_s), \quad (6)$$

where k_i is a negative constant and $U_i(t) = e^{-\alpha \tau_i(t)} [\sum_{j=1}^N (\bar{a}_{ij} \times \Theta_i(y_i(t) - y_j(t))) + \bar{b}_i \Theta_i y_i(t)]$. As defined in [23], $\delta(\cdot)$ represents the Dirac function. $\{t_s\}_{s \in \mathbb{N}}$ is an increasing (stopping time) impulsive sequence with $t_0 \neq 0$ and it will be determined later by (8) and (9). $y_i(t)$ is right continuous with left limits at impulsive instants t_s , i.e., $y_i(t_s) = y_i(t_s^+)$.

Remark 6: Compared to controllers that rely on the system's original states (see, e.g., [27], [28]), PETIC in this paper is based on the virtual state $y_i(t)$ with the same dimension, which facilitates the comparison of states between adjacent agents. Additionally, the energy consumption $\tau_i(t)$ is incorporated into PETIC. Due to the exponential decay property of $e^{-\alpha \tau_i(t)}$, the system can achieve stability more easily.

Let $y(t) = [y_1^T(t), y_2^T(t), \dots, y_N^T(t)]^T$. Then, stochastic MAS (5) is derived as

$$\begin{cases} dy(t) = [\Phi C \Theta y(t) + \Phi f(t)]dt \\ \quad + \Phi D \Theta y(t) d\omega(t), \quad t \neq t_s, \\ y(t) = e^{-\alpha \Gamma(t)} K \tilde{H} \Phi \Theta y(t^-) + y(t^-), \quad t = t_s, \end{cases} \quad (7)$$

where

$$\begin{aligned} f(t) &= [f_1^T(t), f_2^T(t), \dots, f_N^T(t)]^T, \\ \Phi &= \text{diag}\{\Phi_1, \Phi_2, \dots, \Phi_N\}, \\ \Theta &= \text{diag}\{\Theta_1, \Theta_2, \dots, \Theta_N\}, \\ C &= \text{diag}\{C_1, C_2, \dots, C_N\}, \\ D &= \text{diag}\{D_1, D_2, \dots, D_N\}, \\ \tilde{H} &= I_m \otimes H, \quad K = I_m \otimes \text{diag}\{k_1, k_2, \dots, k_N\}, \\ \Gamma(t) &= I_m \otimes \text{diag}\{\tau_1(t), \tau_2(t), \dots, \tau_N(t)\}. \end{aligned}$$

Given the sampling period Δ , PETM is designed as

$$t_0 = \min_{\iota \in \mathbb{N}^+} \{\iota \Delta : W(y(\iota \Delta)) > \psi_1 W(y(0))\}, \quad (8)$$

$$t_{s+1} = t_s + \min_{\iota \in \mathbb{N}^+} \{\iota \Delta : W(y(t_s + \iota \Delta)) > \psi_2 W(y(t_s))\}, \quad (9)$$

where $W(y(t)) = e^{\gamma t} y^T(t) P y(t)$, constants $\gamma > 0$, $\psi_1 \geq 1$, $\psi_2 \geq 1$ and $P \in \mathbb{R}^{mN \times mN}$ is a positive definite matrix.

Remark 7: Compared to the traditional PETMs in [26], [27], [30], this paper takes into account systems' virtual states $y(t)$. Additionally, we adopt the periodic observations to generate a minimum inter-event time Δ , which avoids the Zeno phenomenon.

In what follows, we propose two necessary assumptions that play a crucial role in the proof of Theorem 1.

Assumption 5: Suppose that the energy consumption $\tau_i(t)$ satisfies $\tau_i(t) \geq \tau$.

Remark 8: In Assumption 5, τ represents the minimum energy consumption of the agent. Under PETIC (6), the agent can achieve stability only when its energy consumption is higher than the minimum energy consumption. Under Assumption 5, we have $e^{-\alpha \tau_i(t)} \leq e^{-\alpha \tau}$, which is necessary for the proof of Theorem 1.

Assumption 6: Suppose that

$$2\alpha\tau - \ln\psi_2 - \ln\lambda_1 - \lambda\Delta > 0,$$

where $L_f = \text{diag}\{L_{f_1} I_m, L_{f_2} I_m, \dots, L_{f_N} I_m\}$, $\lambda = \max\{0, \lambda_{\max}([P\Phi C \Theta + (\Phi C \Theta)^T P + (\Phi D \Theta)^T P \Phi D \Theta + P^T P + (L_f \Theta)^T L_f \Theta]P^{-1})\}$ and $\lambda_1 = \lambda_{\max}((e^{\alpha\tau} I_{mN} + K \tilde{H} \Phi \Theta)^T P (e^{\alpha\tau} I_{mN} + K \tilde{H} \Phi \Theta)P^{-1})$.

Remark 9: Let $\bar{\gamma} = \frac{2\alpha\tau - \ln\psi_2 - \ln\lambda_1 - \lambda\Delta}{\Delta}$. Under Assumption 6, we know $\bar{\gamma} > 0$. Choose a constant $\gamma \in (0, \bar{\gamma}]$, we have $\psi_2 \lambda_1 e^{(\lambda+\gamma)\Delta - 2\alpha\tau} \leq 1$, which is important for the proof of Theorem 1. Moreover, it is evident that if other parameters are fixed, then the larger the value of α , the larger the value of $\bar{\gamma}$. In other words, α is useful for adjusting the convergence speed of the system.

Now, we are ready to state the main results on the stabilization of system (7) under PETIC.

Theorem 1: Under Assumptions 1-6, system (7) satisfies $\mathbb{E}|y(t)|^2 \leq M e^{-\gamma t} \mathbb{E}|y(0)|^2$, where M and γ are positive constants.

Proof. Select a Lyapunov function $V(y(t)) = y^T(t) P y(t)$. By Itô's formula and Assumption 3, we have

$$\begin{aligned} \mathcal{L}V(y(t)) &= y^T(t) [P \Phi C \Theta + (\Phi C \Theta)^T P \\ &\quad + (\Phi D \Theta)^T P \Phi D \Theta] y(t) + 2y^T(t) P \Phi f(t) \\ &\leq y^T(t) [P \Phi C \Theta + (\Phi C \Theta)^T P \\ &\quad + (\Phi D \Theta)^T P \Phi D \Theta + P^T P + (L_f \Theta)^T L_f \Theta] y(t) \\ &\leq \lambda V(y(t)). \end{aligned} \quad (10)$$

Since $W(y(t)) = e^{\gamma t} y^T(t) P y(t)$, we obtain

$$\frac{d\mathbb{E}W(y(t))}{dt} = \mathbb{E}\mathcal{L}W(y(t)) \leq (\lambda + \gamma) \mathbb{E}W(y(t)).$$

For $t \in [t_s + l\Delta, t_s + (l+1)\Delta]$, $l \in \mathbb{N}$, using the comparison principle, we get

$$\begin{aligned} \mathbb{E}W(y(t)) &\leq e^{(\lambda+\gamma)(t-t_s-l\Delta)} \mathbb{E}W(y(t_s + l\Delta)) \\ &\leq e^{(\lambda+\gamma)\Delta} \mathbb{E}W(y(t_s + l\Delta)). \end{aligned} \quad (11)$$

When $l = 0$, applying system (7) and Assumption 5, (11) can be derived as

$$\begin{aligned} \mathbb{E}W(y(t)) &\leq e^{(\lambda+\gamma)\Delta} \mathbb{E}W(y(t_s)) \\ &= e^{(\lambda+\gamma)\Delta + \gamma t_s} \mathbb{E}[y^T(t_s^-) (I_{mN} + e^{-\alpha \Gamma(t_s)} K \tilde{H} \Phi \Theta)^T P \\ &\quad \times (I_{mN} + e^{-\alpha \Gamma(t_s)} K \tilde{H} \Phi \Theta) y(t_s^-)] \\ &\leq \lambda_1 e^{(\lambda+\gamma)\Delta - 2\alpha\tau} \mathbb{E}W(y(t_s^-)). \end{aligned} \quad (12)$$

When $l \in (0, l_s)$, $l_s = \max\{\iota \in \mathbb{N}^+ : t_s + \iota\Delta < t_{s+1}\}$. According to PETM (9) and Assumption 5, (11) implies

$$\begin{aligned} \mathbb{E}W(y(t)) &\leq e^{(\lambda+\gamma)\Delta} \mathbb{E}W(y(t_s + l\Delta)) \\ &\leq \psi_2 e^{(\lambda+\gamma)\Delta} \mathbb{E}W(y(t_s)) \\ &\leq \psi_2 \lambda_1 e^{(\lambda+\gamma)\Delta - 2\alpha\tau} \mathbb{E}W(y(t_s^-)). \end{aligned} \quad (13)$$

When $t \in [t_s + l_s \Delta, t_{s+1})$, similar to (13), we have

$$\begin{aligned} \mathbb{E}W(y(t)) &\leq e^{(\lambda+\gamma)\Delta} \mathbb{E}W(y(t_s + l_s \Delta)) \\ &\leq \psi_2 \lambda_1 e^{(\lambda+\gamma)\Delta - 2\alpha\tau} \mathbb{E}W(y(t_s^-)). \end{aligned} \quad (14)$$

Since $\psi_2 \geq 1$, it follows from (12), (13) and (14) that for $t \in [t_s, t_{s+1})$,

$$\mathbb{E}W(y(t)) \leq \psi_2 \lambda_1 e^{(\lambda+\gamma)\Delta - 2\alpha\tau} \mathbb{E}W(y(t_s^-)). \quad (15)$$

According to Assumption 6 and $\gamma \in (0, \bar{\gamma}]$, (15) implies $\mathbb{E}W(y(t)) \leq \mathbb{E}W(y(t_s^-))$. Thus, for $t \geq t_0$, we obtain

$$\begin{aligned} \mathbb{E}W(y(t)) &\leq \mathbb{E}W(y(t_s^-)) \leq \mathbb{E}W(y(t_{s-1}^-)) \\ &\leq \dots \leq \mathbb{E}W(y(t_0^-)). \end{aligned} \quad (16)$$

Then, for $t \in [t_0 - \Delta, t_0)$, applying the comparison principle and PETM (8), we can reveal that

$$\begin{aligned} \mathbb{E}W(y(t)) &\leq e^{(\lambda+\gamma)\Delta} \mathbb{E}W(y(t_0^- - \Delta)) \\ &\leq \psi_1 e^{(\lambda+\gamma)\Delta} \mathbb{E}W(y(0)). \end{aligned} \quad (17)$$

Combining (16) and (17), for $t \geq 0$, we have $\mathbb{E}W(y(t)) \leq \psi_1 e^{(\lambda+\gamma)\Delta} \mathbb{E}W(y(0))$. It is evident that $\lambda_{\min}(P)|y(t)|^2 \leq V(y(t)) \leq \lambda_{\max}(P)|y(t)|^2$. Then, we know

$$\mathbb{E}|y(t)|^2 \leq M e^{-\gamma t} \mathbb{E}|y(0)|^2,$$

where $M = \psi_1 e^{(\lambda+\gamma)\Delta} \frac{\lambda_{\max}(P)}{\lambda_{\min}(P)}$. Therefore, system (7) is mean-square exponentially stable. This completes the proof of Theorem 1. \square

B. PETIC with actuation delay

The controller with actuation delay is designed as

$$\tilde{u}_i(t) = \sum_{s=1}^{\infty} \tilde{k}_i \tilde{U}_i(t) \delta(t - t_s), \quad (18)$$

where $\tilde{U}_i(t) = e^{-\alpha\tau_i(t)} [\sum_{j=1}^N [\bar{a}_{ij} \Theta_i(y_i(t - \tau_s) - y_j(t - \tau_s))] + \bar{b}_i \Theta_i y_i(t - \tau_s)]$, $\tilde{k}_i \in \mathbb{R}$ is a constant and $\tau_s \geq 0$ is the actuation delay. $\{t_s\}_{s \in \mathbb{N}}$ is also determined by (8) and (9) with $t_0 \neq 0$. Then, system (7) can be rewritten as

$$\begin{cases} dy(t) = [\Phi C \Theta y(t) + \Phi f(t)] dt \\ \quad + \Phi D \Theta y(t) d\omega(t), \quad t \neq t_s, \\ y(t) = e^{-\alpha\Gamma(t)} \tilde{K} \tilde{H} \Phi \Theta y(t^- - \tau_s), \quad t = t_s, \end{cases} \quad (19)$$

where $\tilde{K} = I_m \otimes \text{diag}\{\tilde{k}_1, \tilde{k}_2, \dots, \tilde{k}_N\}$.

Remark 10: Compared to PETIC (6), the control input $\tilde{u}_i(t)$ of PETIC (18) is constructed based on the virtual state $y_i(t - \tau_s)$ at the actual impulsive control execution instants. This approach prevents control ineffectiveness caused by the mismatch between the designed control gain and the actual system state. When the actuation delay $\tau_s = 0$, PETIC (18) degenerates into PETIC (6). Furthermore, unlike the control gain k_i in PETIC (6), which must be negative, the \tilde{k}_i in PETIC (18) is not subject to this strict constraint. This flexibility in gain selection expands the applicable scenarios of the control strategy.

Next, we introduce three necessary assumptions that play a vital role in achieving the stabilization of system (19).

Assumption 7: Suppose that the energy consumption $\tau_i(t)$ satisfies $\tau_i(t) \geq \beta_i t$, where β_i is a positive constant.

Remark 11: Based on [20], β_i denotes the minimum power of each agent. Different from PETIC (6), which requires the energy consumption $\tau_i(t) \geq \tau$, under PETIC (18), the system can achieve stability when the energy consumption satisfies $\tau_i(t) \geq 0$. Under Assumption 7, we have $e^{-\alpha\tau_i(t)} \leq e^{-\alpha\beta_i t}$, which is necessary for the proofs of Theorem 2.

Assumption 8: Suppose that the actuation delay τ_s satisfies $\tau_s < \Delta$, $s \in \mathbb{N}$.

Remark 12: Assumption 8 describes a typical scenario of control delays under PETC (see [31]). Under Assumption 8, actual control instants always lie between two adjacent triggering instants.

Assumption 9: Suppose that

$$(2\alpha\beta - \lambda)\Delta - \ln\psi_2 - \ln\tilde{\lambda}_1 > 0,$$

where $\beta = \max\{\beta_1, \beta_2, \dots, \beta_N\}$ and $\tilde{\lambda}_1 = \lambda_{\max}((\tilde{K} \tilde{H} \Phi \Theta)^T P (\tilde{K} \tilde{H} \Phi \Theta) P^{-1})$.

Remark 13: Let $\bar{\gamma}' = \frac{(2\alpha\beta - \lambda)\Delta - \ln\psi_2 - \ln\tilde{\lambda}_1}{2\Delta}$. Based on Assumption 9, we know $\bar{\gamma}' > 0$. Choose a constant $\gamma \in (0, \bar{\gamma}')$, we have $\psi_2 \tilde{\lambda}_1 e^{(\lambda+2\gamma-2\alpha\beta)\Delta} \leq 1$.

Now, we are prepared to introduce the main results on the stabilization of system (19) under PETIC with actuation delays.

Theorem 2: Under Assumptions 1-4 and 7-9, system (19) satisfies $\mathbb{E}|y(t)|^2 \leq M e^{-\gamma t} \mathbb{E}|y(0)|^2$, where M and γ are positive constants.

Proof. Similar to the proof of Theorem 1 for $t \in [t_s + l\Delta, t_s + (l+1)\Delta]$, it is easy to know $\mathbb{E}W(y(t)) \leq e^{(\lambda+\gamma)\Delta} \mathbb{E}W(y(t_s + l\Delta))$. When $l = 0$, based on system (19) and Assumption 7, we have

$$\begin{aligned} & \mathbb{E}W(y(t)) \\ & \leq e^{(\lambda+\gamma)\Delta} \mathbb{E}W(y(t_s)) \\ & = e^{(\lambda+\gamma)\Delta + \gamma t_s} \mathbb{E}[y^T(t_s^- - \tau_s) (e^{-\alpha\Gamma(t_s)} \tilde{K} \tilde{H} \Phi \Theta)^T P \\ & \quad \times (e^{-\alpha\Gamma(t_s)} \tilde{K} \tilde{H} \Phi \Theta) y(t_s^- - \tau_s)] \\ & \leq \tilde{\lambda}_1 e^{(\lambda+\gamma)\Delta - 2\alpha\beta t_s + \gamma\tau_s} \mathbb{E}W(y(t_s^- - \tau_s)). \end{aligned} \quad (20)$$

When $l \in (0, l_s)$, according to PETM (9) and Assumption 7, we get

$$\begin{aligned} & \mathbb{E}W(y(t)) \\ & \leq e^{(\lambda+\gamma)\Delta} \mathbb{E}W(y(t_s + l\Delta)) \\ & \leq \psi_2 e^{(\lambda+\gamma)\Delta} \mathbb{E}W(y(t_s)) \\ & \leq \psi_2 \tilde{\lambda}_1 e^{(\lambda+\gamma)\Delta - 2\alpha\beta t_s + \gamma\tau_s} \mathbb{E}W(y(t_s^- - \tau_s)). \end{aligned} \quad (21)$$

As a matter of fact, (21) is not only tenable for $t \in [t_s + l\Delta, t_s + (l+1)\Delta]$ but also suitable for $t \in [t_s + l_s\Delta, t_{s+1})$.

According to $\psi_2 \geq 1$, $t_s \geq \Delta$ and Assumption 8, it follows from (20) and (21) that for $t \in [t_s, t_{s+1})$,

$$\begin{aligned} & \mathbb{E}W(y(t)) \\ & \leq \psi_2 \tilde{\lambda}_1 e^{(\lambda+\gamma)\Delta - 2\alpha\beta t_s + \gamma\tau_s} \mathbb{E}W(y(t_s^- - \tau_s)) \\ & \leq \psi_2 \tilde{\lambda}_1 e^{(\lambda+2\gamma-2\alpha\beta)\Delta} \mathbb{E}W(y(t_s^- - \tau_s)). \end{aligned} \quad (22)$$

Based on Assumption 9 and $\gamma \in (0, \bar{\gamma}')$, (22) implies $\mathbb{E}W(y(t)) \leq \mathbb{E}W(y(t_s^- - \tau_s))$. Similar to (16), for $t \geq t_0$, we have $\mathbb{E}W(y(t)) \leq \mathbb{E}W(y(t_0^- - \tau_0))$.

Under Assumption 8, we know $t_0^- - \tau_0 \in [t_0 - \Delta, t_0)$. Then, applying (17), we obtain $\mathbb{E}|y(t)|^2 \leq M e^{-\gamma t} \mathbb{E}|y(0)|^2$. Therefore, this completes the proof of Theorem 2. \square

Remark 14: Different from MASs investigated in [11], [12], [13], [14], [15], [16], we consider a fully heterogeneous stochastic MAS with a time-varying topology. In this paper, a virtual state space is constructed to unify the dimensions of the agents and ensure information interaction between them. Furthermore, based on the energy consumption in the time-varying topology, this paper proposes a novel PETM that conserves bandwidth resources. Finally, by designing PETICs with/without actuation delays, the consensus of the system is achieved.

IV. NUMERICAL SIMULATION

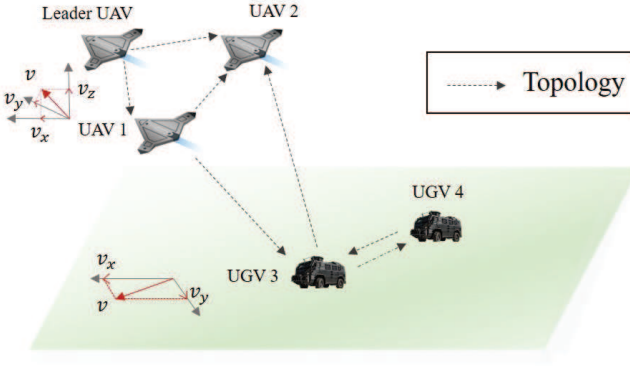


Fig. 2. UAVs-UGVs system.

In this section, we consider a leader-following system, where the leader is an UAV and the followers consist of two UAVs and two UGVs. The topological diagram is shown as Fig. 2. Based on the work in [36], we incorporate stochastic noise into the system. Then, the dynamic leader model is described as

$$\begin{aligned} d\eta_0(t) &= v_0(t)dt + d_0v_0(t)d\omega(t), \\ dv_0(t) &= [c_{\eta_0}\eta_0(t) + c_{v_0}v_0(t)]dt \\ &\quad + [d_{\eta_0}\eta_0(t) + d_{v_0}v_0(t)]d\omega(t), \quad t \geq 0, \end{aligned}$$

where $\eta_0(t) = [\eta_{0x}^T(t), \eta_{0y}^T(t), \eta_{0z}^T(t)]^T \in \mathbb{R}^3$ and $v_0(t) = [v_{0x}^T(t), v_{0y}^T(t), v_{0z}^T(t)]^T \in \mathbb{R}^3$ are the position and the velocity of leader UAV. Let $\bar{x}_0(t) = [\eta_0^T(t), v_0^T(t)]^T$, the leader system is established as

$$d\bar{x}_0(t) = \mathbb{C}_0\bar{x}_0(t)dt + \mathbb{D}_0\bar{x}_0(t)d\omega(t), \quad t \geq 0,$$

where $\mathbb{C}_0 \in \mathbb{R}^{6 \times 6}$ and $\mathbb{D}_0 \in \mathbb{R}^{6 \times 6}$.

In what follows, a dynamic follower model is established as

$$\begin{aligned} d\eta_i(t) &= v_i(t)dt + d_i v_i(t)d\omega(t), \\ dv_i(t) &= [c_{\eta_i}\eta_i(t) + c_{v_i}v_i(t) + f_i(\eta_i(t))]dt \\ &\quad + [d_{\eta_i}\eta_i(t) + d_{v_i}v_i(t)]d\omega(t), \quad i \in \mathcal{N}, \quad t \geq 0, \end{aligned}$$

where $\mathcal{N} = \{1, 2, 3, 4\}$, $\eta_i(t) = [\eta_{ix}^T(t), \eta_{iy}^T(t), \eta_{iz}^T(t)]^T \in \mathbb{R}^3$ and $v_i(t) = [v_{ix}^T(t), v_{iy}^T(t), v_{iz}^T(t)]^T \in \mathbb{R}^3$, $i = 1, 2$, are the position and the velocity of UAVs. $\eta_i(t) = [\eta_{ix}^T(t), \eta_{iy}^T(t)]^T \in \mathbb{R}^2$ and $v_i(t) = [v_{ix}^T(t), v_{iy}^T(t)]^T \in \mathbb{R}^2$, $i = 3, 4$, are the position and the velocity of UGVs. Let $\bar{x}_i(t) = [\eta_i^T(t), v_i^T(t)]^T$, we constructed the following systems:

$$d\bar{x}_i(t) = [\mathbb{C}_i\bar{x}_i(t) + \bar{f}_i(\bar{x}_i(t)) + \bar{u}_i(t)]dt + \mathbb{D}_i\bar{x}_i(t)d\omega(t), \quad i \in \mathcal{N}, \quad t \geq 0,$$

where $\bar{f}_i(\bar{x}_i(t)) = [\mathbf{0}, f_i(\bar{x}_i(t))]^T$, $\bar{u}_i(t) = [\mathbf{0}, u_i(t)]^T$, $\mathbb{C}_i \in \mathbb{R}^{6 \times 6}$ and $\mathbb{D}_i \in \mathbb{R}^{6 \times 6}$.

Let $\bar{z}_i(t) = \bar{x}_i(t) - \Xi_i\bar{x}_0(t) - \bar{x}_i^*$ and $\bar{y}_i(t) = \Phi_i\bar{z}_i(t)$, where \bar{x}_i^* denotes the desired relative position and $\bar{x}_i^* = [\bar{x}_{xi}^T, \bar{x}_{yi}^T, \bar{x}_{zi}^T, \mathbf{0}, \mathbf{0}, \mathbf{0}]^T$. It is easy to obtain that

$$\begin{aligned} d\bar{y}_i(t) &= [\Phi_i\mathbb{C}_i\bar{y}_i(t) + \Phi_i\bar{f}_i(t) + \Phi_i\bar{u}_i(t)]dt \\ &\quad + [\Phi_i\mathbb{D}_i\Theta_i\bar{y}_i(t) + \Phi_i\mathbb{D}_i\bar{x}_i^*]d\omega(t), \quad i \in \mathcal{N}, \quad t \geq 0, \end{aligned}$$

where $\bar{f}_i(t) = \bar{f}_i(\bar{z}_i(t)) + \mathbb{C}_i\bar{x}_i^*$ and $|\Phi_i\mathbb{D}_i\Theta_i\bar{y}_i(t) + \Phi_i\mathbb{D}_i\bar{x}_i^*| \leq L_{D_i}|\bar{y}_i(t)|$.

Then, the dynamic parameters matrix of UAVs-UGVs system can be described as:

$$\begin{aligned} \mathbb{C}_0 &= \text{diag} \left\{ \begin{bmatrix} 0 & 1 \\ 0 & 0 \end{bmatrix}, \begin{bmatrix} 0 & 1 \\ 0 & 0 \end{bmatrix}, \begin{bmatrix} 0 & 1 \\ -0.05 & 0.05 \end{bmatrix} \right\}, \\ \mathbb{D}_0 &= \text{diag} \left\{ \begin{bmatrix} 0 & 0.01 \\ 0 & 0 \end{bmatrix}, \begin{bmatrix} 0 & 0.01 \\ 0 & 0 \end{bmatrix}, \begin{bmatrix} 0 & 0.01 \\ 0 & 0 \end{bmatrix} \right\}, \\ H &= \begin{bmatrix} 1 & 0 & 0 & 0 \\ 1 & -1 & 1 & 0 \\ 1 & 0 & -2 & 1 \\ 0 & 0 & 1 & -1 \end{bmatrix}. \end{aligned}$$

For $i = 1, 2$,

$$\begin{aligned} \mathbb{C}_i &= \text{diag} \left\{ \begin{bmatrix} 0 & 1 \\ -0.9 & 0.9 \end{bmatrix}, \begin{bmatrix} 0 & 1 \\ 0.6 & 0.6 \end{bmatrix}, \begin{bmatrix} 0 & 1 \\ -0.01 & 0.01 \end{bmatrix} \right\}, \\ \mathbb{D}_i &= \text{diag} \left\{ \begin{bmatrix} 0 & 1.5 \\ 0.6 & 0.6 \end{bmatrix}, \begin{bmatrix} 0 & 1.9 \\ 1.6 & 1.6 \end{bmatrix}, \begin{bmatrix} 0 & 1.7 \\ 0.6 & 0.6 \end{bmatrix} \right\}, \end{aligned}$$

$\Xi_i = \Phi_i = \Theta_i = I_6$, $\bar{f}_i(t) = [0, 0, 0, 0.5\sin(0.3\eta_{ix}(t)), 0.7 \times \sin(0.5\eta_{iy}(t)), 0.5\sin(0.9\eta_{iz}(t))]^T$, $\bar{x}_1^* = [3, 3, 0, 0, 0, 0]^T$ and $\bar{x}_2^* = [0, 3, 0, 0, 0, 0]^T$. Based on [20], [21], we normalize the parameters to obtain the energy consumption $\tau_i(t) = \tau + 0.005t$.

For $i = 3, 4$,

$$\begin{aligned} \mathbb{C}_i &= \text{diag} \left\{ \begin{bmatrix} 0 & 1 \\ -0.8 & 0.8 \end{bmatrix}, \begin{bmatrix} 0 & 1 \\ -0.6 & 0.6 \end{bmatrix} \right\}, \\ \mathbb{D}_i &= \text{diag} \left\{ \begin{bmatrix} 0 & 1.5 \\ 1.2 & 1.2 \end{bmatrix}, \begin{bmatrix} 0 & 1.9 \\ 0.5 & 0.5 \end{bmatrix} \right\}, \\ \Xi_i = \Theta_i &= \begin{bmatrix} 1 & 0 & 0 & 0 & 0 & 0 \\ 0 & 1 & 0 & 0 & 0 & 0 \\ 0 & 0 & 0 & 1 & 0 & 0 \\ 0 & 0 & 0 & 0 & 1 & 0 \end{bmatrix}, \quad \Phi_i = \begin{bmatrix} 1 & 0 & 0 & 0 \\ 0 & 1 & 0 & 0 \\ 0 & 0 & 0 & 0 \\ 0 & 0 & 1 & 0 \\ 0 & 0 & 0 & 1 \\ 0 & 0 & 0 & 0 \end{bmatrix}, \end{aligned}$$

$$\bar{f}_i(t) = [0, 0, 0.5\sin(0.3\eta_{ix}(t)), 0.7\sin(0.5\eta_{iy}(t))]^T, \quad \bar{x}_3^* = [2, 2, 0, 0]^T, \quad \bar{x}_4^* = [0, 0, 0, 0]^T \text{ and } \tau_i(t) = \tau + 0.0047t.$$

Remark 15: Different from [36], we introduce stochastic noise into the system, which more accurately reflects the actual situation. In a stochastic operating environment, the agents we consider exhibit characteristics across multiple dimensions. Thus, we can achieve the coordinated operation of UAVs and UGVs. Such coordinated operations of UAVs and UGVs have also been applied and verified in [37], [38]. However, it should be noted that neither of these studies takes stochastic noise into account. Due to the unobservable nature of stochastic noise, achieving information transmission between adjacent heterogeneous agents becomes challenging. This difficulty also demonstrates the necessity of constructing the virtual state space proposed in this paper.

The simulation is performed by MATLAB with step = 0.003. The initial values are given as follows:

$$\begin{aligned}\eta_0(0) &= [1.55, -1.5, 10.01]^T, v_0(t) = [2.3, -3.15, 1.1]^T, \\ \eta_1(0) &= [7.11, -2.78, 2.4]^T, v_1(0) = [2, 1.52, 0.51]^T, \\ \eta_2(0) &= [10.12, 7.63, 2.6]^T, v_2(0) = [-0.5, -1.02, 1.3]^T, \\ \eta_3(0) &= [10.51, -7.7]^T, v_3(0) = [2, -2.92]^T, \\ \eta_4(0) &= [5.12, 5.63]^T, v_4(0) = [1.5, -3.02]^T.\end{aligned}$$

Then, Fig. 3 and Fig. 4 illustrate the trajectories of UAVs-UGVs system without control. It can be seen that uncontrolled system is not stable.

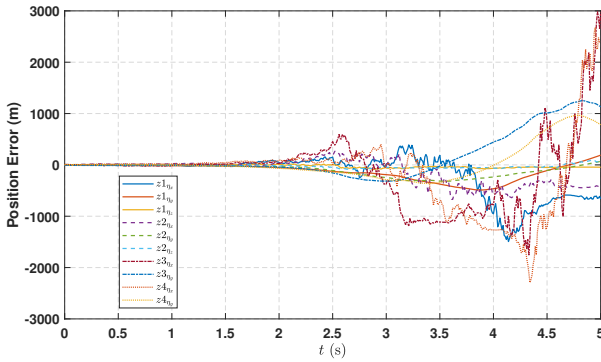


Fig. 3. Position errors without control.

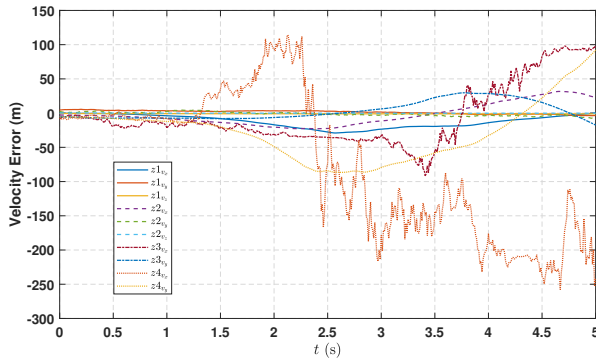


Fig. 4. Velocity errors without control.

First, we consider the case of control without actuator delays:

$$\bar{u}_i(t) = \sum_{s=0}^{\infty} k_i \bar{U}_i(t) \delta(t - t_s), \quad (23)$$

where $\bar{U}_i(t) = e^{-\alpha \tau_i(t)} [\sum_{j=1}^N (\bar{a}_{ij} \Theta_i (\bar{y}_i(t) - \bar{y}_j(t))) + \bar{b}_i \Theta_i \bar{y}_i(t)]$.

According to system (7), to verify the effectiveness of PETIC (23), we choose parameters $k_1 = -1.51$, $k_2 = -2.38$, $k_3 = -3.41$, $k_4 = -1.10$, $\alpha = 12.34$, $\tau = 0.003$, $\psi_1 = 1.4$, $\psi_2 = 1.001$, $\Delta = 0.009$ and $P = 0.95I_{24}$. By calculation, we obtain $\lambda = 10.99$, $\lambda_1 = 0.98$, which indicates that Assumption 6 is satisfied. Furthermore, we choose $\gamma = 0.0019$ such that $\psi_2 \lambda_1 e^{(\lambda+\gamma)\Delta-2\alpha\tau} \leq 1$. Therefore, all conditions in Theorem 1 are satisfied.

Then, we draw the following figures. Fig. 5(a) depicts the trajectory of the virtual state $y(t)$ under PETIC (23). Figs. 5(c), 5(d), 5(e) and 5(f) represent the state errors $z(t)$ of the four followers. Fig. 5(b) plots the triggering intervals. Fig. 6 presents the dynamic operating trajectories of UAVs and UGVs during 20s. Based on these figures, it can be observed that the virtual states effectively reflect the movements of states with different dimensions. Meanwhile, it is evident that the state errors of UAVs and UGVs quickly achieve mean-square exponential stabilization under PETIC (23). Compared to the fixed-period control that requires 556 controller updates, the number of updates is only 294 by PETIC (23), resulting in a 48% reduction in data transmissions. Also, the Zeno behavior does not occur.

Second, we consider the case of control with actuator delays:

$$\tilde{u}_i(t) = \sum_{s=1}^{\infty} \tilde{k}_i \tilde{U}_i(t) \delta(t - t_s), \quad (24)$$

where $\tilde{U}_i(t) = e^{-\alpha \tau_i(t)} [\sum_{j=1}^N (\bar{a}_{ij} \Theta_i (y_i(t - \tau_s) - y_j(t - \tau_s))) + \bar{b}_i \Theta_i y_i(t - \tau_s)]$.

According to system (19), we choose parameters $\tau_s = 0.04$, $\tilde{k}_1 = -0.71$, $\tilde{k}_2 = 0.55$, $\tilde{k}_3 = 0.08$, $\tilde{k}_4 = -0.32$, $\alpha = 2000$, $\tau = 0$, $\beta = 0.0047$, $\psi_1 = 1.2$, $\psi_2 = 1.1$, $\Delta = 0.09$ and $P = 0.5I_{24}$. By calculation, we obtain $\lambda = 8.19$, $\lambda_1 = 1.16$, which indicates that Assumption 9 is satisfied. Based on Remark 13, we get $\bar{\gamma}' = 0.031$. Then, we choose $\gamma = 0.03$. So, all conditions in Theorem 2 are satisfied.

Fig. 7(a) shows the behaviour of the virtual state $y(t)$ under PETIC (24) with actuation delays. Figs. 7(c), 7(d), 7(e) and 7(f) plot the state errors $z(t)$. Fig. 7(b) presents the time intervals of control with actuation delays. Fig. 8 depicts the dynamic operating trajectories of UAVs and UGVs. From these figures, it can be seen that UAVs and UGVs overcome the influence of actuator delays and achieve stability. What's more, in comparison with the fixed-period control that required about 55 updates, the proposed PETIC (24) achieves a 71% reduction in updating frequency, requiring only 16 updates.

V. CONCLUSIONS AND FUTURE RESEARCH PROSPECTS

Different from the traditional stochastic MASs, the time-varying topology with energy consumption is considered in this paper. To address the problem of dimension discrepancy among agents, a virtual state is introduced. Based on them, we propose novel PETICs with/without actuation delays to achieve the mean-square exponential consensus of the systems. According to these control schemes, we have achieved the consensus operation of UAVs and UGVs in simulations. In the future work, we will study a class of heterogeneous stochastic MASs with sampled-data outputs and design ETCs based on observers.

REFERENCES

- [1] Y. Luo, F. Tang, H. Zhang and D. Yang, "Synchronous position-attitude loop regulation-based distributed optimal trajectory tracking control for multi-UAVs formation with external disturbances," *IEEE Trans. Syst., Man, Cybern., Syst.*, vol. 54, no. 12, pp. 7445–7456, Dec. 2024.

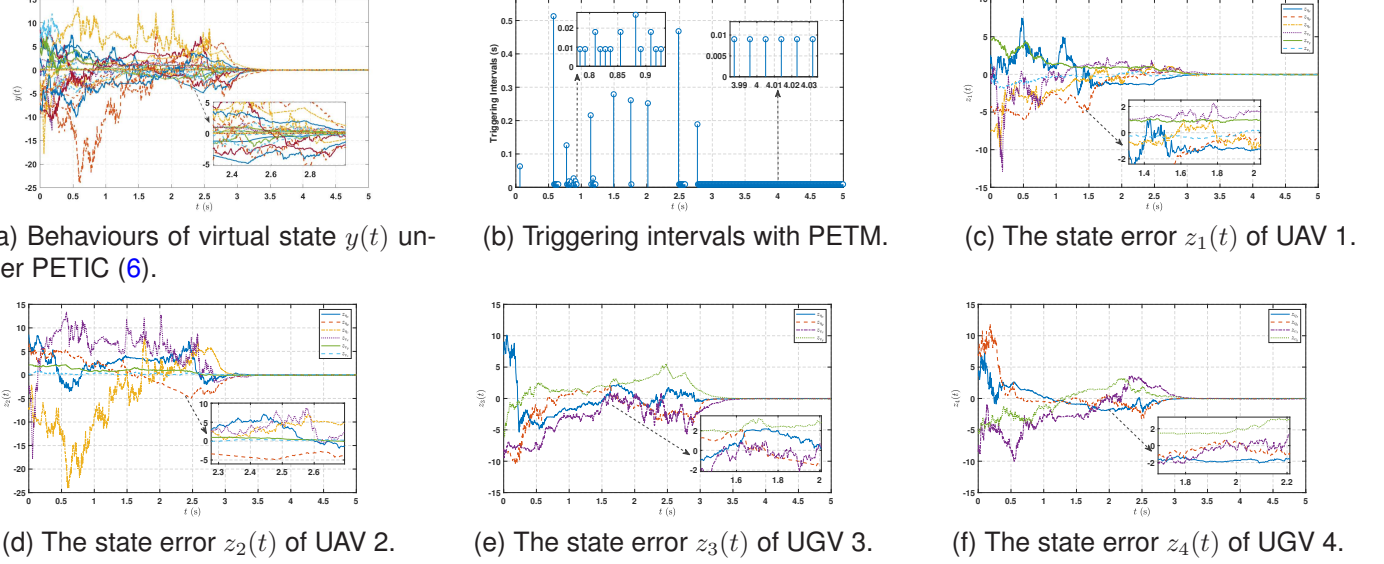


Fig. 5. Simulation results of UAVs and UGVs under PETIC (6) without actuation delays.

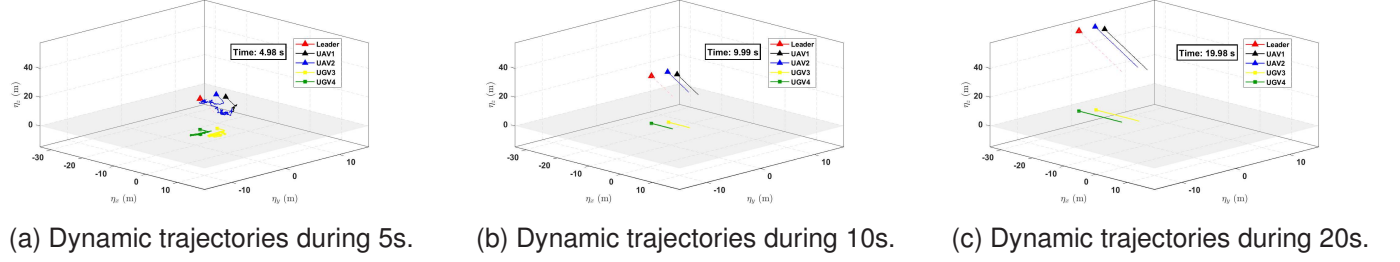


Fig. 6. Dynamic trajectories of UAVs and UGVs under PETIC (6) without actuation delays.

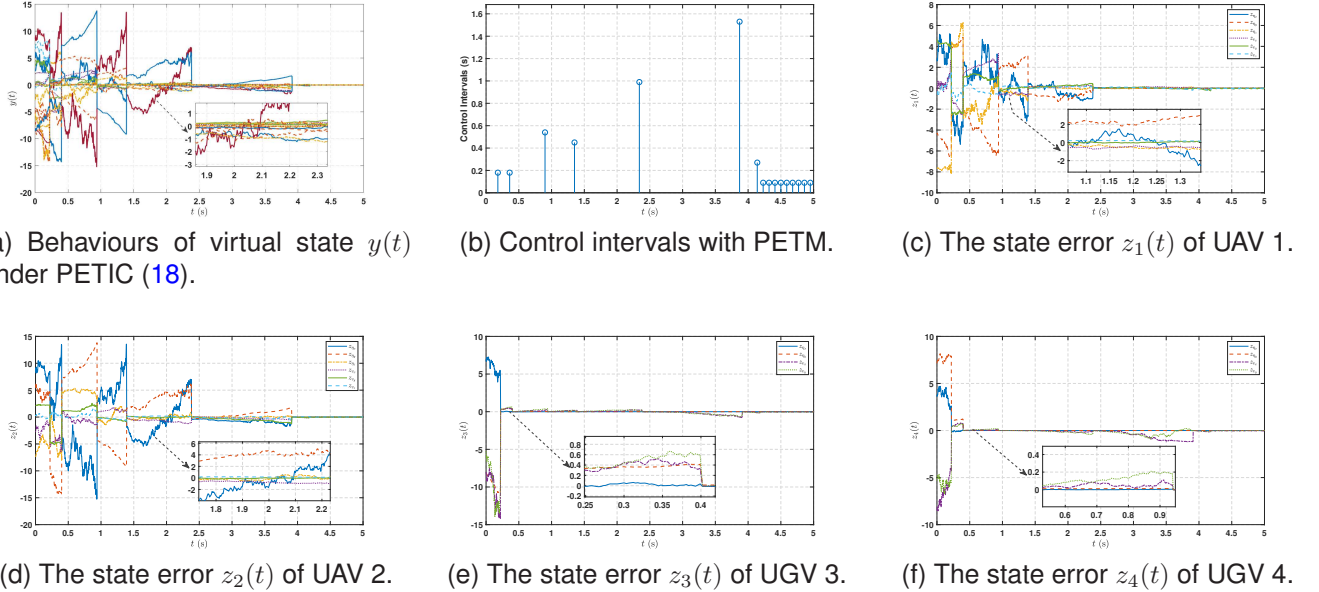
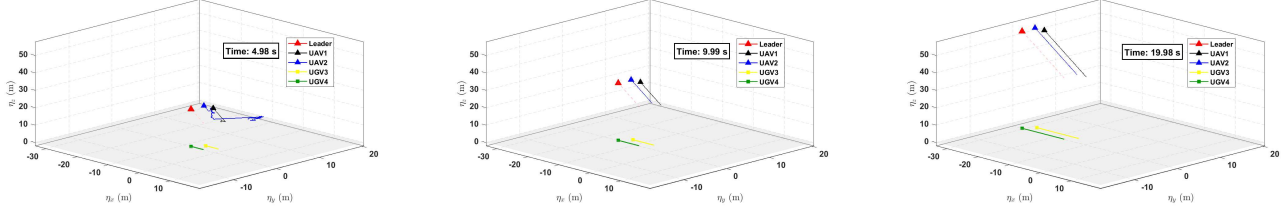


Fig. 7. Simulation results of UAVs and UGVs under PETIC (18) with actuation delays.

[2] X. Zheng, S. Yu, H. Cao, T. Shi, S. Xue and T. Ding, "Sensitivity-based heterogeneous ordered multi-agent reinforcement learning for distributed

volt-var control in active distribution network," *IEEE Trans. Smart Grid.*, vol. 16, no. 3, pp. 2115–2126, May 2025.



(a) Dynamic trajectories during 5s. (b) Dynamic trajectories during 10s. (c) Dynamic trajectories during 20s.

Fig. 8. Dynamic trajectories of UAVs and UGVs under PETIC (18) with actuation delays.

[3] Z. Wang, L. Wang, H. Zhang, L. Vlacic and Q. Chen, "Distributed formation control of nonholonomic wheeled mobile robots subject to longitudinal slippage constraints," *IEEE Trans. Syst., Man, Cybern., Syst.*, vol. 51, no. 5, pp. 2992–3003, May 2021.

[4] G. Zhang, C. Liang and Q. Zhu, "Adaptive fuzzy event-triggered optimized consensus control for delayed unknown stochastic nonlinear multi-agent systems using simplified ADP," *IEEE Trans. Autom. Sci. Eng.*, vol. 22, no. 0, pp. 11780–11793, Feb. 2025.

[5] B. Zhang, L. Cai, F. Deng and S. Xie, "Consensus of multi-agent systems via aperiodically intermittent sampling stochastic noise," *IEEE Trans. Circuits Syst I Regul Pap.*, vol. 71, no. 3, pp. 1311–1323, Mar. 2024.

[6] W. Sun, B. Li, A. Wu, W. Guo and X. Wu, "The event-triggered impulsive controls for quasisynchronization of the leader-following heterogeneous dynamical networks," *IEEE Trans. Cybern.*, vol. 53, no. 10, pp. 6277–6288, Oct. 2023.

[7] L. You, X. Jiang, B. Li, X. Zhang and H. Yan, "Impulsive layered control of heterogeneous multi-agent systems under limited communication," *IEEE Trans. Ind. Informatics*, vol. 20, no. 3, pp. 5014–5021, Mar. 2024.

[8] H. Wang and J. Dong, "Neural network-based hierarchical fault-tolerant affine formation control for heterogeneous nonlinear multi-agent systems," *IEEE Trans. Intell. Transp. Syst.*, vol. 25, no. 5, pp. 4503–4511, May 2024.

[9] X. Guo, P. Liu, Z. Wu, D. Zhang and C. Ahn, "Hybrid event-triggered group consensus control for heterogeneous multiagent systems with TVNUD faults and stochastic FDI attacks," *IEEE Trans. Automat. Control*, vol. 68, no. 12, pp. 8013–8020, Dec. 2023.

[10] F. Wang, J. Deng, Z. Liu and Z. Chen, "A modular event-triggered containment control scheme for nonlinear heterogeneous multiagent systems with unknown leaders," *IEEE Trans. Intell. Transp. Syst.*, vol. 54, no. 7, pp. 4190–4203, Jul. 2024.

[11] J. Han, H. Zhang, Y. Wang, and H. Ren, "Output consensus problem for linear heterogeneous multiagent systems with dynamic event-based impulsive control," *IEEE Trans. Syst., Man, Cybern., Syst.*, vol. 53, no. 1, pp. 334–345, Jan. 2023.

[12] S. Luo, X. Xu, L. Liu, and G. Feng, "Leader-following consensus of heterogeneous linear multiagent systems with communication time-delays via adaptive distributed observers," *IEEE Trans. Cybern.*, vol. 52, no. 12, pp. 13336–13349, Dec. 2022.

[13] A. Koru, A. Ramirez, S. Sarsilmaz, R. Sipahi, T. Yucelen and K.M. Dogan, "Containment control of multi-human multi-agent systems under time delays," *IEEE Trans. Syst., Man, Cybern., Syst.*, vol. 54, no. 6, pp. 3344–3356, Jun. 2024.

[14] Y. Yao, Y. Luo, J. Cao, A. Li and D. Yue, "Finite-time prescribed performance H_∞ control of multi-agent systems based on sample-data event-triggered mechanism," *IEEE Trans. Autom. Sci. Eng.*, vol. 22, no. 0, pp. 20341–20353, Aug. 2025.

[15] H. Hu, Q. Zhu and M. Hou, "Constraint-coupled distributed coordination control for nonlinear stochastic multiagent systems: application to power resource allocation," *IEEE Trans. Syst., Man, Cybern., Syst.*, vol. 55, no. 8, pp. 5520–5530, Aug. 2025.

[16] K. Li, L. Song and Y. Li, "Fuzzy adaptive resilient output control for nonlinear multi-agent systems under byzantine agents," *IEEE Trans. Autom. Sci. Eng.*, vol. 22, no. 0, pp. 8783–8793, Nov. 2024.

[17] J. Zhu, G. Zhuang, X. Xie and J. Xia, "Distributed dual-terminal adaptive triggered consensus tracking of descriptor multi-agent systems against asynchronous DoS attacks with markov switching topologies," *IEEE Trans. Circuits Syst I Regul Pap.*, vol. 71, no. 12, pp. 6265–6278, Dec. 2024.

[18] J. Wang, G. Wen and Z. Duan, "Distributed antiwindup consensus control of heterogeneous multiagent systems over markovian randomly switching topologies," *IEEE Trans. Automat. Control*, vol. 67, no. 11, pp. 6310–6317, Nov. 2022.

[19] Z. Feng, M. Huang, D. Wu, E. Wu and C. Yuen, "Multi-agent reinforcement learning with policy clipping and average evaluation for UAV-assisted communication markov game," *IEEE Trans. Intell. Transp. Syst.*, vol. 24, no. 12, pp. 14281–14293, Dec. 2023.

[20] A. Bavand, S.A. Khajehhoddin, M. Ardakan and A. Tabesh, "Online estimations of li-ion battery SOC and SOH applicable to partial charge/discharge," *IEEE Trans. Transp. Electrif.*, vol. 8, no. 3, pp. 3673–3685, Sep. 2022.

[21] H. Yan, Y. Chen and S. Yang, "UAV-enabled wireless power transfer with base station charging and UAV power consumption," *IEEE Trans. Veh. Technol.*, vol. 69, no. 11, pp. 12883–12896, Nov. 2020.

[22] Z. Yang, S. Bi and Y. Zhang, "Dynamic offloading and trajectory control for UAV-enabled mobile edge computing system with energy harvesting devices," *IEEE Trans. Commun.*, vol. 21, no. 12, pp. 10515–10528, Dec. 2022.

[23] Z. Hu and X. Mu, "Impulsive consensus of stochastic multi-agent systems under semi-Markovian switching topologies and application," *Automatica*, vol. 150, pp. 110871, Dec. 2023.

[24] X. Li, Y. Xing and S. Song, "Nonlinear impulsive control for stability of dynamical systems," *Automatica*, vol. 178, pp. 112371, Aug. 2025.

[25] J. Lu, B. Jiang and W. Zheng, "Potential impacts of delay on stability of impulsive control systems," *IEEE Trans. Automat. Control*, vol. 67, no. 10, pp. 5179–5190, Oct. 2022.

[26] B. Jiang, J. Wei, Y. Liu and W. Gui, "Periodic event-triggered impulsive control of linear uncertain systems," *IEEE Trans. Autom. Sci. Eng.*, vol. 22, no. 0, pp. 6876–6883, Sep. 2024.

[27] J. Ping, S. Zhu, W. Luo and Z. Zhang, "Hyper-exponential stabilization of neural networks by event-triggered impulsive control with actuation delay," *IEEE Trans. Neural Netw. Learn. Syst.*, vol. 36, no. 4, pp. 7778–7781, Apr. 2025.

[28] Z. Zhang, S. Peng, D. Liu, Y. Wang and T. Chen, "Leader-following mean-square consensus of stochastic multiagent systems with ROUs and RONs via distributed event-triggered impulsive control," *IEEE Trans. Cybern.*, vol. 52, no. 3, pp. 1836–1849, Mar. 2022.

[29] K. Zhang and E. Braverman, "Event-triggered impulsive control for nonlinear systems with actuation delays," *IEEE Trans. Automat. Control*, vol. 68, no. 1, pp. 540–547, Jan. 2023.

[30] Z. Hu and X. Mu, "Event-triggered impulsive control for stochastic networked control systems under cyber attacks," *IEEE Trans. Syst., Man, Cybern., Syst.*, vol. 52, no. 9, pp. 5636–5645, Sep. 2022.

[31] W. Zhang, J. Chen, S. Wen and T. Huang, "Event-triggered random delayed impulsive consensus of multi-agent systems with time-varying delay," *IEEE Trans. Syst., Man, Cybern., Syst.*, vol. 9, no. 2, pp. 2059–2064, Apr. 2025.

[32] X. Ruan, J. Feng, C. Xu, J. Wang and Y. Zhao, "Dynamic event-triggered pinning synchronization for switched impulsive complex networks with asynchronous switching," *IEEE Trans. Circuits Syst. II-Express Briefs*, vol. 69, no. 4, pp. 2211–2215, Apr. 2022.

[33] T. Zhang, J. Cao and X. Li, "Prescribed-time control of switched systems: an event-triggered impulsive control approach," *IEEE Trans. Syst., Man, Cybern., Syst.*, vol. 54, no. 7, pp. 4284–4293, Jul. 2024.

[34] W. Sun, Z. Yuan, Z. Lu, J. Hu and S. Chen, "Quasisynchronization of heterogeneous neural networks with time-varying delays via event-triggered impulsive controls," *IEEE Trans. Cybern.*, vol. 52, no. 5, pp. 3855–3866, May 2022.

[35] X. Yang, Q. Zhu, and H. Wang, "Exponential stabilization of stochastic systems via novel event-triggered switching controls," *IEEE Trans. Autom. Control*, vol. 69, no. 11, pp. 7948–7955, Nov. 2024.

- [36] B. Shi, S. Wu and B. Wei, "Neural-network-based event-triggered formation tracking for nonlinear multi-uav systems with switching topologies under dos attacks," *IEEE Trans. Autom. Sci. Eng.*, vol. 22, no. 0, pp. 11656–11667, Feb. 2025.
- [37] Y. Li and Y. Li, "Resilient distributed fixed-time tracking of heterogeneous UAVs-UGVs systems against DoS attacks," *IEEE Trans. Syst., Man, Cybern., Syst.*, vol. 54, no. 9, pp. 5780–5790, Sep. 2024.
- [38] Z. Xiao, H. Xu, J. Tao, R. Lu and P. Shi, "Leader-following formation of heterogeneous multi-agent systems with time-varying topology: a virtual neighbor framework," *IEEE Trans. Syst., Man, Cybern., Syst.*, vol. 22, no. 0, pp. 21341–21352, Sep. 2025.